Journal of Non-Crystalline Solids 71 (1985) 171–185
North-Holland, Amsterdam

Section VI. Sol-gel processes

STRUCTURAL EVOLUTION DURING THE GEL TO GLASS CONVERSION *

C.J. BRINKER [1], E.P. ROTH [1], G.W. SCHERER [2] and D.R. TALLANT [1]

[1] *Sandia National Laboratories* **, *Albuquerque, New Mexico 87185, USA*
[2] *Corning Glass Works, Corning, New York 14830, USA*

We have used differential scanning calorimetry (DSC) to measure quantitatively enthalpic changes which accompany gel densification and have related these changes to the evolving gel structure using Raman spectroscopy, gas adsorption, and thermal analysis. We show that the network structure, which results principally from skeletal dehydration (via condensation) during gel densification, is considerably different from the melt-glass structure. A dramatic reduction in viscosity and the formation of metastable M–O–M bonds as a product of condensation reactions are examples of these differences. Despite the complex manner in which the gel evolves toward a glass, once the gel has been densified and heated above T_g, its structure and properties, e.g. viscosity and distribution of relaxation times, become indistinguishable from those of the conventionally melted glass.

1. Introduction

In "sol–gel" processes based on metal alkoxide syntheses a macromolecular network forms as a result of condensation reactions:

$$\begin{array}{l} \mathrm{RO} \\ \mathrm{RO}\!\gtrdot\!\mathrm{Si{-}OH} \\ \mathrm{RO} \end{array} + \mathrm{HO{-}Si}\!\lessdot\!\begin{array}{l} \mathrm{OR} \\ \mathrm{OR} \\ \mathrm{OR} \end{array} \rightarrow \begin{array}{l} \mathrm{RO} \\ \mathrm{RO}\!\gtrdot\!\mathrm{Si{-}O{-}Si} \\ \mathrm{RO} \end{array}\!\lessdot\!\begin{array}{l} \mathrm{OR} \\ \mathrm{OR} \\ \mathrm{OR} \end{array} + \mathrm{H_2O} \qquad (1)$$

where R≡H, Si or C_xH_{2x+1}. The network structure depends on the degree of hydrolysis and the catalytic conditions employed. Recently, it has been established that under many conditions of gel synthesis single phase polymeric networks rather than two phase colloidal sols result [1–3]. Gelation "freezes-in" this ramified polymeric structure which at the gel point is considerably less crosslinked (on average fewer bridging oxygen linkages per network former) than colloidal gels or, of course, the corresponding melted glass. Continued crosslinking occurs during desiccation and the subsequent conversion of the porous xerogel to a dense glass. However, virtually all of these additional crosslinks result from condensation reactions, so that the resulting network

* This work partially performed at Sandia National Laboratories supported by the US Department of Energy under contract number DE-AC04-76DP00789.
** A US DOE facility.

0022-3093/85/$03.30

structure can be viewed as essentially a product of dehydration (eq. (1)). Since gels are densified without melting at temperatures often less than or equal to the T_g of the corresponding melt-prepared glass, the following questions arise: do structural variations "frozen-in" at the gel point or network structures resulting from dehydration differ from melt-prepared glass structures? If so, to what temperature do these structural variations persist?

In answer to this latter question, Mackenzie [4] compared reported physical and structural properties of densified gels and melt-derived glasses (e.g. density, refractive index, hardness and expansion coefficient). Although Mackenzie concluded that based on these comparisons the overall structure and properties of sol–gel glasses must be similar to melt-formed glasses, the recent results of numerous experimental observations on gel derived glasses suggest otherwise. Some of these observations are summarized as follows:

(1) the devitrification of melted sodium-silicate gels results in different phases and/or differing amounts of a particular phase compared to the conventional melted glass [5].
(2) The apparent viscosity of a gel-derived SiO_2 glass at 1800°C depends on the molar ratio of H_2O : Si used during the gelation process [6].
(3) The viscosity of gel-derived soda lime silica glass remains lower than that of the conventional glass after 150 h of melting [7].
(4) The kinetics and thermodynamics of phase separation in melted gel-derived soda-silica glass are different than the conventional glass [8] and are affected by the gel preparation and heat treatment procedure.
(5) The solid phase density (skeletal density) of porous gels (SiO_2, [9] sodium borosilicate [10], and a multicomponent aluminoboro-silicate [11]) is less than that of the conventional glass. (In one case [10] $\rho_{skeleton}/\rho_{glass} = 0.63$).
(6) The intensities of "so-called" defect bands, D_1 and D_2, in Raman spectra of porous, silicate gels are considerably greater than in conventional fused silica, whereas the intensities of D_1 and D_2 in densified silica gels are sometimes less than in conventional fused silica [12,13].

Some of these results may be attributable to differences in oxide composition or hydroxyl contents (e.g. (1)–(4) above); however, it was claimed that (2) and (3) resulted from structural rather than compositional differences. If differences do exist between melt and gel-derived glasses, as suggested by the above observations, the implication is that the network structure which results from gelation or from dehydration is different than the structure which forms during the thermodynamic equilibrium established in the melt. Therefore, one goal of this investigation was to obtain thermodynamic and structural information as the gel densified to a glass, in order to compare the evolving gel structure to that of a conventionally melted glass. Secondly, since the idea of structural variations persisting well above the glass transition temperature is contrary to established theories of structural relaxation in glass, a second goal of this investigation was to compare the structures of densified gels to melted glass and determine whether the densified gel structure changed during heat treatments above T_g.

2. Experimental

2.1. Sample preparation

Silica (samples A2 and B2) and multicomponent borosilicate gels (samples BS1 and BS2) were prepared using multi-step hydrolysis procedures as described in refs. [2] and [11] (for compositions see table 1). In every case, the first step consisted of hydrolyzing tetraethylorthosilicate (TEOS) with 1 mol. H_2O/mol. Si under acidic conditions. This is known to result in a distribution of weakly branched oligomers which undergo further hydrolysis and condensation during subsequent hydrolysis steps [2]. Power law analyses of small angle X-ray scattering (SAXS) curves were used to confirm that at or near the gel point each system investigated consisted of rather weakly crosslinked polymeric macromolecules rather than agglomerated colloidal silica particles [1,2,14]. Thus, at the gel point fully crosslinked regions of dense "glass-like" structure do not exist even on a microscopic scale (10–1000 Å).

Cylindrical specimens were prepared by casting in polypropylene molds followed by gelation and drying at 50°C. For comparison, composition BS2 was also made by conventional melting at 1600°C in a closed Pt crucible.

2.2. Methods of analysis

Thermal analytical techniques including thermal gravimetric analysis, dilatometry, and differential scanning calorimetry were used in combination to measure physical, chemical and enthalpic changes which accompanied gel densification [15,11]. Surface area and pore volume were determined by analyses of nitrogen adsorption isotherms at 77 K [15,11]. Structural information was obtained by in-situ Raman spectroscopy at temperatures up to 700°C in a flowing helium atmosphere. Residual hydroxyl contents of densified gels were determined by transmission infrared spectroscopy at 3660 cm^{-1} [15].

3. Results and discussion

In the first three parts of this section, we present evidence concerning the evolving structure of the gel as it transforms into a dense glass at temperatures

Table 1
Compositions investigated (wt%). BS1 and BS2 measured by inductively coupled plasma spectroscopy

	SiO_2	B_2O_3	Al_2O_3	Na_2O	BaO	OH(ppm)
A2	100	–	–	–	–	
B2	100	–	–	–	–	
BS1	74.5	12.5	5.2	5.4	2.1	3197
BS2	86.1	12.0	1.06	0.90	–	182
BS2 (melt)	85.3	12.9	1.02	0.96	–	256

less than or equal to the T_g of the corresponding melted glass. In the final part of this section we compare the glass transition behavior of a densified gel to that of its corresponding melt prepared glass after heat treatments above T_g.

3.1. Structural relaxation

Since a gel is not a product of melting, the concept of fictive temperature is ill-defined. However, it is reasonable to assume that the ramified structure "frozen-in" at the gel point results in a desiccated network structure which is considerably more open (exhibiting greater excess free volume and thus lower skeletal density) than in a melt-prepared glass and thus may be described by an effective high fictive temperature. If this view is correct, upon subsequent heat treatment the skeletal density would increase exothermically at a temperature near T_g by diffusive motion of the polymeric network without expulsion of water or other by-products, i.e. by structural relaxation [16]. To determine whether the concepts of fictive temperature and structural relaxation were applicable to gels, we performed a series of measurements on the silica gel, A2, which, of the gels investigated, was the most ramified (least highly cross linked) at the gel point as determined by SAXS [1,2].

Fig. 1 shows changes in weight loss, shrinkage, and surface area for A2 heated at 2°C/min in air. Fig. 2 shows bulk density (calculated from the measured values of shrinkage and weight loss) and skeletal density calculated using the following relationship:

$$V_p = \frac{1}{\rho_{bulk}} - \frac{1}{\rho_{skeleton}}, \tag{2}$$

where V_p is the measured specific pore volume. The skeletal density is therefore defined as the density of the solid phase which is not penetrated by the

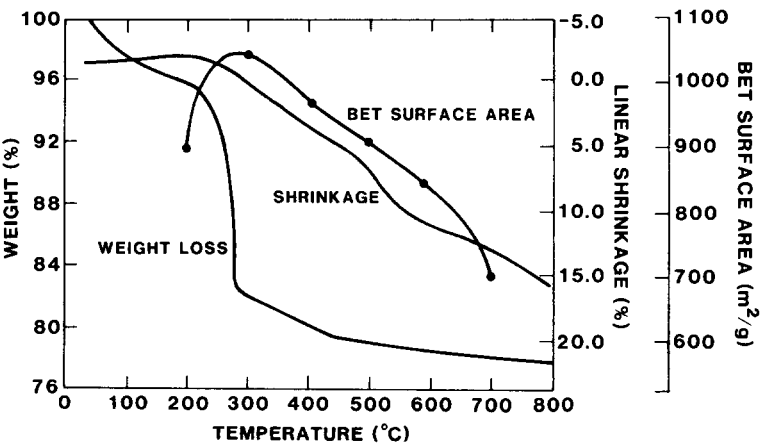

Fig. 1. Weight loss, shrinkage, and BET surface area for A2 heated at 2°C/min in air.

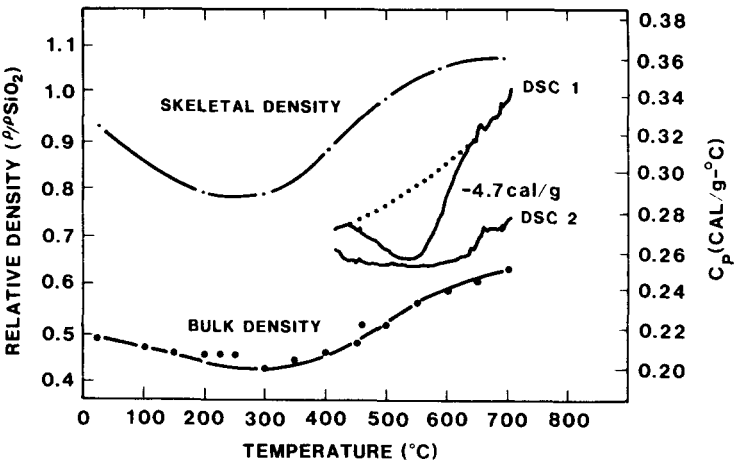

Fig. 2. Calculated bulk density and skeletal densities and first and second DSC scans, DSC-1 and DSC-2, respectively for A2. Relative densities above 1.0 result from errors associated with the measurements of V_p and ρ_{bulk}.

adsorbate gas. Also plotted in fig. 2 is a DSC scan (400 to 700°C) of A2 which had been previously heated to 400°C in air to remove all physically adsorbed water (DSC-1) and a repeat scan (400 to 700°C) performed after cooling the specimen to 400°C at 80°C/min (DSC-2).

The skeletal density is observed to decrease initially owing to desorption of physically adsorbed water and solvents from the gel surface and pyrolysis of unhydrolyzed alkoxy groups, resulting in an apparent increase in surface area [9]. Above about 275°C, the skeleton densifies causing shrinkage and reduction in surface area. Initially shrinkage is accompanied by substantial weight loss which suggests that the skeleton is first densifying primarily by a condensation process (e.g. eq. (1)). However, above 400°C a sharp inflection is observed in the shrinkage curve over a temperature range in which the skeleton densifies appreciably with no increase in the rate of weight loss. DSC-1 shows that this inflection is accompanied by an exotherm. The repeat scan, DSC-2, shows that the process associated with the exotherm is irreversible.

The decrease in surface area ($\sim 200\ m^2/g$ between 400 and 650°C) can be explained by the reduction in surface area expected from skeletal densification:

$$\left(\frac{\rho_{\text{skeleton}_{(\text{initial})}}}{\rho_{\text{skeleton}_{(\text{final})}}}\right)^{2/3} = \frac{S_{\text{final}}}{S_{\text{initial}}} \tag{3}$$

proving that the shrinkage does not result from the sintering of open porosity. To prove that shrinkage results from structural relaxation, it is necessary to account for the enthalpic contributions of: (1) the change in surface energy, (2) the heat of dehydration (the sum of the heat of formation of Si–O–Si bonds plus the heat of vaporization of the condensation product, water), (3) the heat

capacity of the skeleton, and (4) structural changes (if any) toward a more thermodynamically stable structure (i.e. structural relaxation). The measured exotherm from 400–650°C, −4.7 cal/g, is more negative than the sum of the energy due to the reduction in BET surface area (−9.6 cal/g, assuming an average surface energy of 0.048 cal/m^2 (200 erg/cm^2) for a partially hydroxylated silica surface [17]) and the endothermic contributions of the heat of dehydration and the skeletal heat capacity (> 7 cal/g, see section 3.2). Thus, structural relaxation appears to be consistent with the experimental observations. One might argue that viscous sintering of isolated pores existing within the skeleton also explains these observations (removal of these pores would cause an exothermic densification of the skeleton without contributing to the BET surface area). However, a previous study of A2 gels showed that the average diameter of pores involved in viscous sintering above 700°C is 2.3 nm [9]. Since the rate of viscous sintering is inversely proportional to the product of pore size and viscosity, the pores responsible for equivalent shrinkage rates at ~ 400°C, where the viscosity is expected to be higher, must be smaller than 2.3 nm. Thus, the dimension of these "pores" would approach the scale of free volume and their removal would be indistinguishable from structural relaxation.

Whether one views this process as occurring by structural relaxation or viscous sintering, it is certain that the viscosity of the skeleton must be sufficiently reduced to allow structural rearrangements (i.e. relaxation or viscous flow). This implies that the onset of the glass transition of the silicate skeleton is initially dramatically reduced from that of vitreous silica (> 1100°C) and that only upon further heating does the T_g approach that of the melt-prepared glass (by continued crosslinking and/or additional structural relaxation). The reduced viscosity and skeletal density are expected to be general properties of desiccated gels; however, it should be noted that the exothermic behavior associated with the inflection in the shrinkage curve has thus far only been observed for gels prepared under conditions favoring growth of weakly crosslinked polymers in solution and which, therefore, are expected to contain the greatest free volume when desiccated.

3.2. Metastable polymerization

The previous section examined densification behavior resulting from structural ramifications "frozen-in" at the gel point. This section will address the question: what is the network structure which results from dehydration of the skeleton? In colloidal silica gels composed of anhydrous silica particles, this question is of little practical importance. However in most gels prepared from metal alkoxides, the complete network structure evolves as dehydration proceeds.

We performed two sets of experiments in order to obtain thermodynamic and structural information regarding the dehydrated gel structure. The first experiment was performed to determine the heat of formation of M–O–M

bonds resulting from dehydration. The heat of formation is very sensitive to the M–O–M bond angle, ϕ. Revesz and Gibbs [18] performed ab initio molecular orbital (MO) calculations to determine the energies of disiloxane molecules as a function of ϕ. The minimum energy value occurred at $\phi = 144°$ which is close to the most probable value of the Si–O–Si angle in vitreous silica, viz. 150° [19]:

$$2H_4SiO_4 \rightarrow H_6Si_2O_7 + H_2O \; \Delta H_{f298K} = -4 \text{ kcal/mol.} \quad (4)$$

According to Galeener [20], the minimum energy corresponds to a structure composed of puckered n-fold rings where $n \geqslant 4$. When ϕ is reduced from its minimum energy value, the calculated energy of the disiloxane molecule increases substantially. For example, when ϕ is reduced to 87°, which is the known value for edge-sharing tetrahedra in the SiS_2 structural form of silica [21] (2-fold rings) the energy increases to 50 kcal/mol. [19].

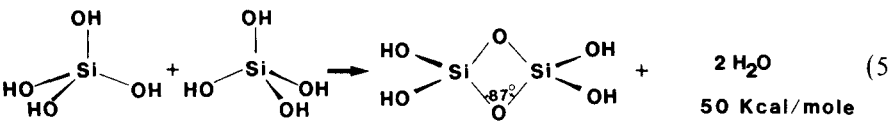

(5)

Although the calculated energy of formation is high, two membered rings have been proposed to explain infrared spectral features at 940, 908, and 888 cm^{-1}, observed when dehydrating colloidal silica at temperatures above 400°C [22].

Because of the sensitivity of the M–O–M bond energy to the ring statistics, a determination of the heat of formation of M–O–M bonds resulting from dehydration should provide information concerning the structure of the dehydrated skeleton. The experiment consisted of preheating pairs of identical samples (the borosilicate composition, BS1) to 525°C in air at heating rates ranging from 0.5 to 30°C/min. After quenching to room temperature, one sample of each set was immediately transferred to a DSC and the other to a TGA. Each sample was brought to thermal equilibrium at 427°C to desorb any physically adsorbed water and heated at 40°C/min to 717°C causing complete densification. The DSC sample was cooled at 80°C/min to 427°C and reheated at 40°C/min to 717°C in order to determine the heat capacity of the skeleton during its glass transition. The residual [OH] contents of the densified gels were determined by infrared spectroscopy assuming an extinction coefficient of 56 l/mol. cm [23].

BET surface area measurements revealed that after the initial heat treatment to 525°C the surface areas of the samples equaled (412 ± 6) m^2/g independent of the heating rate. Thus during the DSC experiment in which the samples are completely densified, the only differences between samples result from differences in enthalpy associated with dehydration of the skeleton (i.e. during densification all samples undergo identical changes in surface area and have nearly identical skeletal heat capacities as inferred from the repeat DSC scan, DSC-2). Figs. 3 and 4 show the TGA and DSC results for samples initially heated at 2 and 30°C/min. The TGA results show that the sample initially

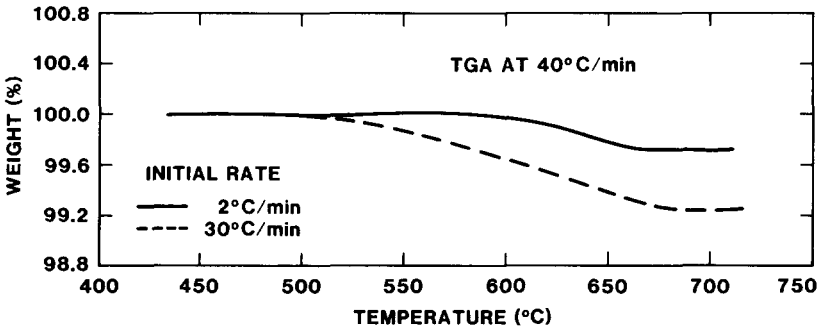

Fig. 3. Weight loss at 40°C/min for BS1 samples originally heated to 525°C at 2 and 30°C/min.

heated at 30°C/min to 525°C undergoes greater weight loss above 525°C. Since physically adsorbed water is removed by 427°C, this additional weight loss can be attributed to a greater number of condensation reactions (e.g. eqs. (1), (4) and (5)).

From the differences in weight loss and specific heat we can easily compute the heat of dehydration. Integrating the difference of the heat capacities, (DSC-1) − (DSC-2), over the temperature limits 525 to 660°C for each initial heating rate gives the heat of dehydration plus the change in surface free energy. Since both samples lose equivalent amounts of surface area, the difference of these two integrals (7.6 − (−7.5 cal/g)) equals the heat of dehydration assuming the surface energy to be the same for each sample. Since the skeletal heat capacities (DSC-2) are almost identical, this same result (~ 15 cal/g) is obtained by integrating the difference between DSC-1 scans. Using 548 cal/g for the heat of vaporization of water and assuming that 1 mol. of water is evolved for each mole of M–O–M bonds formed, the average heat of

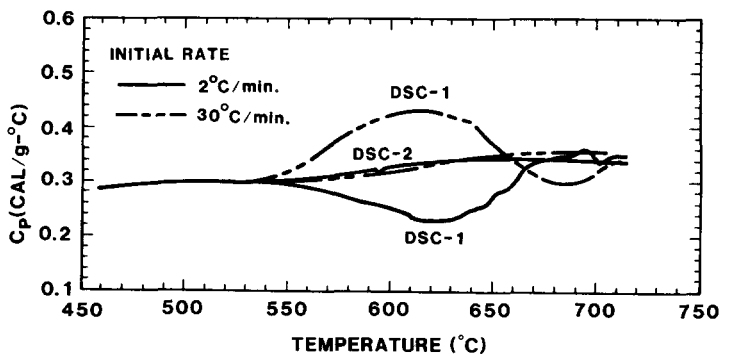

Fig. 4. Initial and repeat DSC scans, DSC-1 and DSC-2, for BS1 samples initially heated to 525°C at 2 and 30°C/min.

formation of M–O–M bonds is calculated to be 15 cal/3.4×10^{-4} mol. or 44.1 kcal/mol.

Making the speculative assumption that the MO calculations are valid to describe surface dehydration and the assumption that the bond energy is relatively insensitive to M (Si, B, or Al) at least for highly strained configurations this result suggests that the majority of M–O–M bonds formed by dehydration above 525°C are highly strained ($\phi \rightarrow 87°$) perhaps as a result of 2-fold ring formation.

The dehydrated gel network is metastable. Above T_g it dissociates exothermically to form more stable M–O–M bonds ($\phi \rightarrow 150°$) as indicated by the exotherms observed above 660°C (the exotherms decreased in proportion to the decreasing amounts of dehydration as the initial heating rate was reduced). However, even at 100°C above T_g all of the energy is not recovered suggesting that these metastable networks persist at temperatures above T_g.

3.3. Raman experiments

Further information concerning the network structure resulting from dehydration was obtained by in situ Raman spectroscopy of the silica gel, B_2, at temperatures up to 700°C. The Raman spectrum of a separate gel sample was obtained at room temperature after complete densification at 1050°C. All of the spectra were compared to the spectrum of commercial fused silica. Figs. 5 and 6 show our results. The broad features of the fused silica spectrum, at about 430, 800, 1065, and 1200 cm^{-1} can be explained quantitatively in terms of a central force dynamical calculation applied to a continuous random network model [20]. The sharp features at 480 cm^{-1} (D_1) and 604 cm^{-1} (D_2) are not explained by this model and have been ascribed to "defects" arising from broken bonds [24], paracrystalline clusters [25], and small planar rings [20].

The most notable feature of the gel spectra is the intensification of D_2 as the temperature is increased from 50°C to 700°C. This has also been observed by Krol and van Lierop [12] and by Gottardi et al. [13] for acid catalyzed silica gels. As seen in fig. 6 the relative intensity of D_2 increases monotonically and the relative intensity of the 3740 cm^{-1} band, assigned to isolated silanols, decreases monotonically over the temperature range 400 to 700°C. Densification (and reduction in surface area) of the gel at 1050°C causes a dramatic reduction in D_2 to a level comparable to that of fused silica.

The Raman bands at 975 and 3740 cm^{-1} have been assigned to non-hydrogen bonded ("isolated") vicinal surface silanol groups [12,26]. If this assignment is valid and if the decrease in the relative intensities of the 975 cm^{-1} and 3740 cm^{-1} bands is not merely coincidental to the increase in the relative intensity of the D_2 band, then it appears that the structure giving rise to D_2 forms on the gel surface as a condensation product of isolated silanols. Molecular models indicate that adjacent silanol groups which condense to form n-fold rings, where $n \geq 3$, can hydrogen bond to each other [27]. However, if the silanols share a common siloxane bridge, they would be

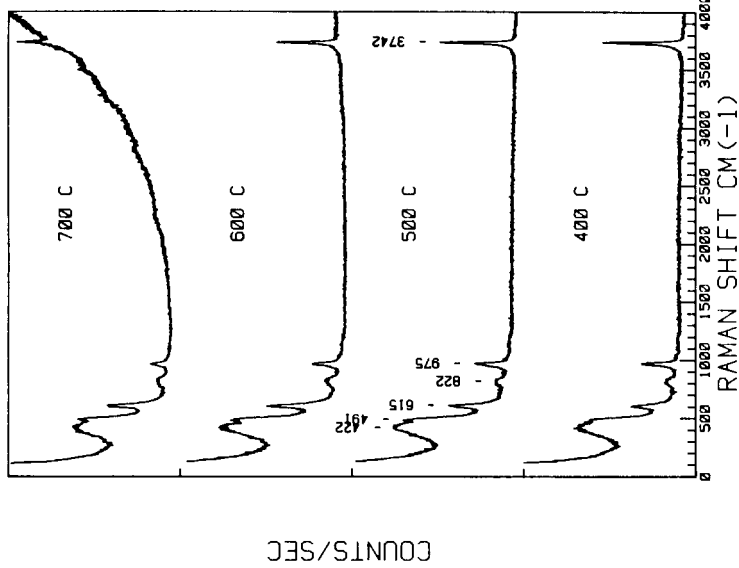

Fig. 6. In situ Raman spectra (*zz*) for B2 at 700, 600, 500 and 400°C.

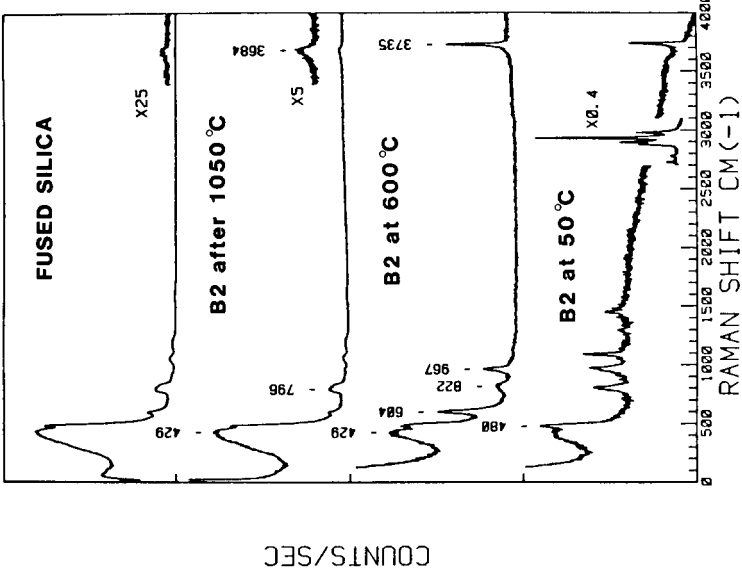

Fig. 5. Raman spectra (*zz*) of (top) vitreous silica (Optasil), B2, the silica gel, densified at 1050°C, B2 measured in situ at 600°C and B2 measured in situ at 50°C.

sufficiently separated to appear as isolated silanols in the Raman spectrum.

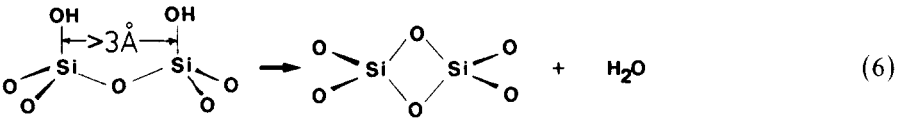

(6)

Thus, one possible explanation for the increased relative intensity of D_2 is the formation of 2-fold rings on the gel surface. This is consistent with IR results reported by Morrow and Cody for the dehydration of colloidal silica [22] and provides an explanation for the unusually high heat of dehydration measured for the borosilicate gel (section 3.2). In addition, these structures readily react with water which is consistent with the reported reactivity of D_2. If 2-fold rings were to form, higher temperature heat treatments would cause their dissociation into lower energy, higher order rings. This is consistent with the dramatic reduction in D_2 observed after the gel is densified at 1050°C by viscous sintering. A second condensation reaction involving isolated silanols is the formation of bridge bonds spanning very small pores during sintering:

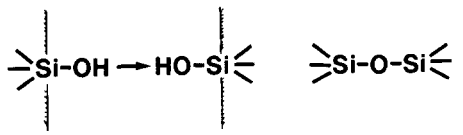

(7)

However, this reaction would result in higher order rings ($n > 2$) which are more stable and thus are less likely to be removed during viscous sintering.

It should be noted that the paracrystalline structure model for the D_2 band requires a geminal silanol group, $=Si(OH_2)$, as a precursor, if it is to be formed by a condensation reaction [25]. Therefore, the validity of the assignments of the 975 and 3740 cm^{-1} to only vicinal silanol groups is crucial to delineating the dehydration mechanism and making a final structural assignment to the D_2 Raman band.

3.4. Gel-glass structure

We have Raman evidence that the densified silica gel structure (B2) is "similar" to the structure of conventional fused silica (fig. 5). However, it is uncertain whether vibrational spectroscopy is sensitive to subtle differences in molecular conformations which might exist between gel and melt-derived glasses. Therefore, we investigated the evolution of enthalpy (H) during the glass transition for a densified gel and melted glass of the same borosilicate composition (BS2).

When a glass is heated from below its glass transition temperature, the heat capacity $(\partial H/\partial T)_p$ initially represents the change in H caused by vibrations of the atoms in their potential wells. As the temperature is increased the atoms

acquire enough energy to break bonds and rearrange into new structures causing the enthalpy to increase more rapidly. This produces an increase in the heat capacity. The difference between the high temperature "liquid" and low temperature "glassy" heat capacities is the structural contribution to H. The "structural" contribution is thought to include changes in the vibrational spectrum caused by changes of the average molecular configuration of the liquid. Thus, the glass transition behavior should be a sensitive probe of the densified gel structure.

Densification of gels under standard laboratory conditions ($\sim$ 50% RH) is known to result in glasses with high hydroxyl contents (e.g. $>$ 20X melted glass [28]). Since OH affects the connectivity of the network and therefore its viscosity, the gel specimens used in this study were dehydrated under vacuum and sintered in desiccated, ultra-high-purity helium at 900°C. The resulting [OH] equalled 83% of that in the melted glass. DSC experiments were performed at 20°C/min on the densified samples after an initial heat treatment at 900, 1100, 1200, 1300, and 1600°C (30 min) followed by cooling from 900°C at 2°C/min. Calibration runs performed before and after each DSC run showed that the calorimeter was within $\pm 2\%$ accuracy over the investigated temperature range.

Heat capacity data (fig. 7) were fit using the model of Debolt et al. [29]. The fitting parameters are T_0, x, Q, and b. T_v is the relaxation time and is proportional to viscosity:

$$T_v = T_0 \exp\left(\frac{xQ}{RT} + \frac{(1-x)Q}{RT_f} \right), \tag{8}$$

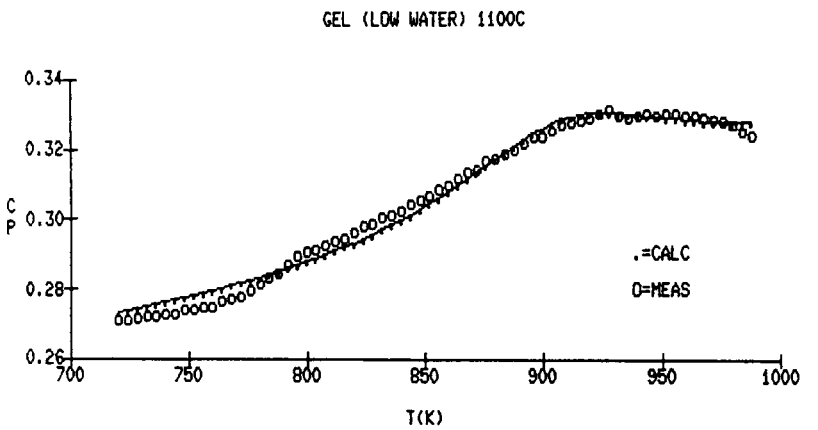

Fig. 7. Measured and calculated heat capacity for densified BS2 after an initial heat treatment at 1100°C followed by cooling from 900°C at 2°C/min.

where Q equals the activation energy for viscous flow, T_f equals the fictive temperature, and x is a constant normally equal to about 0.5. The volume relaxation function, M_v, is expressed by a distribution of relaxation times:

$$M_v = \exp\left[-\left(\int_0^t \frac{dt'}{T_v}\right)^b\right]. \tag{9}$$

The 1100°C data were fitted with the following parameters: $b = 0.22$, $Q = 197$ kcal/mol., $x = 0.4$ and $T_0 = 8.9 \times 10^{-48}$ s (fig. 7). The value of b is exceptionally low indicating a broad distribution of relaxation times which suppresses the normally observed overshoot in C_p above T_g. The value of Q is unusually large as we confirmed by cooling rate experiments which showed a small change in C_p with a large change in the cooling rate.

These same parameters provided excellent fits to the C_p data of the melted glass (fig. 8) and the gel glass previously heated to 1600°C. This shows that within experimental error the gel-glass and the melted glass are indistinguishable for these heat treatments. The C_p curves after 900, 1200, and 1300°C heat treatments were not fit as well using the above parameters. We have no explanation for this inconsistent behavior at present. For all heat treatments an inflection in C_p was observed at ~ 800 K for the gel-derived glasses. Although this behavior is consistent with phase separation, TEM comparisons of the gel and melt-derived glasses showed no differences and no evidence of phase separation in either case.

In our opinion, these results along with the Raman results indicate that, at least after heating to temperatures well above T_g, the structures of gel-derived glass and melted glass are indeed very similar. Additional work is needed to investigate the structure of gels densified at temperatures nearer T_g.

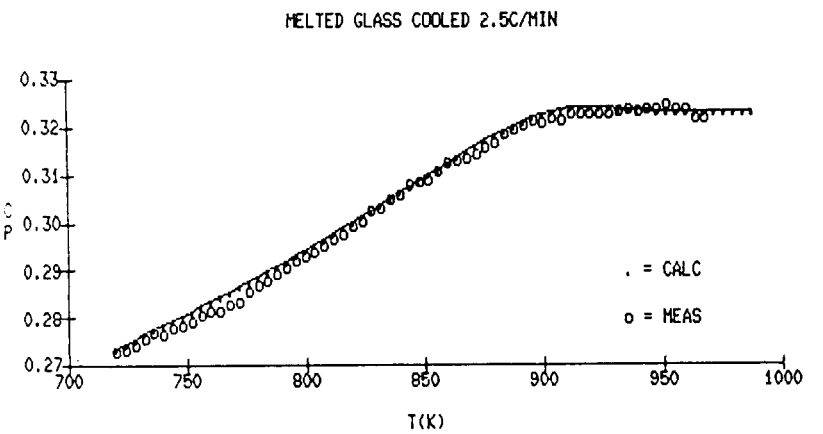

Fig. 8. Measured and calculated heat capacities for melted BS2 after cooling from 900°C at 2.5°C/min (using the same fitting parameters as for fig. 7).

4. Conclusions

The results of our experiments show that as the gel evolves from a macromolecular cluster in solution toward a fully crosslinked "glass" via condensation reactions, the network structure is considerably different from that of a conventionally melted glass. It contains greater free volume, and has enhanced atomic mobility (reduced viscosity). Dehydration above about 400°C results in the formation of energetic M–O–M bonds perhaps due to the formation of metastable 2-fold rings. Despite structural differences prior to densification, the structure (as evidenced by the Raman spectra) and properties (e.g. the glass transition behavior) of gels densified above T_g *can* be indistinguishable from the corresponding melted glass. Further work is needed to confirm that for identical compositions gel and melted glass structures *must* be identical after heat treatments above T_g.

The authors thank C.S. Ashley, T. Tormey, M.C. Oborney, S. Weissman, and T.J. Headley of Sandia National Laboratories for their contributions to this work. We are also indebted to Dave Smith of Corning Glass Works Computer Services Department for developing the fitting routine used to analyze the DSC data.

References

[1] D.W. Schaefer and K.D. Keefer, in: Better Ceramics Through Chemistry, eds., C.J. Brinker, D.E. Clark and D.R. Ulrich (Elsevier–North-Holland, New York, 1984).
[2] C.J. Brinker, K.D. Keefer, D.W. Schaefer, R.A. Assink, B.D. Kay and C.S. Ashley, J. Non-Crystalline Solids 63 (1984) 45.
[3] S. Sakka, K. Kamiya, K. Makita and Y. Yamamoto, J. Non-Crystalline Solids 63 (1984) 223.
[4] J.D. Mackenzie, J. Non-Crystalline Solids 48 (1982) 1.
[5] G.F. Neilson and M.C. Weinberg, J. Non-Crystalline Solids 63 (1984) 365.
[6] B.E. Yoldas, J. Non-Crystalline Solids 63 (1984) 145.
[7] B.E. Yoldas, J. Non-Crystalline Solids 51 (1982) 105.
[8] G.F. Neilson and M.C. Weinberg, in: Materials Processing in the Reduced Gravity Environment of Space, ed., Guy E. Rindone (Elsevier, New York, 1982) p. 333.
[9] C.J. Brinker, W.D. Drotning and G.W. Scherer, in: Better Ceramics Through Chemistry, eds., C.J. Brinker, D.E. Clark and D.R. Ulrich (Elsevier–North-Holland, New York, 1984).
[10] N. Tohge, G.S. Moore and J.D. Mackenzie, J. Non-Crystalline Solids 63 (1984) 95.
[11] C.J. Brinker and G.W. Scherer, submitted to J. Non-Crystalline Solids.
[12] D.M. Krol and J.G. van Lierop, J. Non-Crystalline Solids 63 (1984) 131.
[13] V. Gottardi, M. Guglielmi, A. Bertoluzza, C. Fagnano and M.A. Morelli, J. Non-Crystalline Solids 63 (1984) 71.
[14] K.D. Keefer and C.J. Brinker, to be published.
[15] C.J. Brinker and S.P. Mukherjee, J. Mat. Sci. 16 (1981) 1980.
[16] J. Debast and P. Gilard, Phys. Chem. Glasses 4 (1963) 117.
[17] R.K. Iler, The Chemistry of Silica, (Wiley, New York, 1979).
[18] A.G. Revesz and G.V. Gibbs, in: The Physics of MOS Insulators, eds., G. Lucovsky, S.T. Pantelides and F.L. Galeener (Pergamon, New York, 1980).
[19] G.V. Gibbs, private communication.

[20] F.L. Galeener, J. Non-Crystalline Solids 49 (1982) 53.
[21] V.A. Weiss and A. Weiss, Z. Anorg. Allg. Chem. 95 (1954) 276.
[22] B.A. Morrow and L.A. Cody, J. Phys. Chem. 80 (1976) 2761.
[23] J.P. Williams, Y. Su, W.R. Strezegowski, B.L. Butler, H.L. Hoover and V.O. Altemose, Am. Ceram. Soc. Bull. 55 (1976) 524.
[24] R.H. Stolen, J.T. Krause and C.R. Kurkjian, Disc. Faraday Soc. 50 (1970) 103.
[25] J.C. Phillips, J. Non-Crystalline Solids 63 (1984) 347.
[26] C.A. Murray and T.J. Geytak, Phys. Rev. B20 (1979) 3368.
[27] T.A. Michalske and B.C. Bunker, to be published, J. Appl. Phys.
[28] C.J. Brinker and D.M. Haaland, 1984 Annual Meeting and Exposition of the American Ceramic Soc., Pittsburgh, PA; for abstract see Am. Ceram. Soc. Bull. 63 (1984) 499.
[29] M.A. Debolt, A.J. Easteal, P.B. Macedo and C.T. Moynihan, J. Am. Ceram. Soc. 59 (1976) 16.